

# CONTROL OF CLUSTERED ACTION POTENTIAL FIRING IN A MATHEMATICAL MODEL OF ENTORHINAL CORTEX STELLATE CELLS

Luke Tait<sup>1,2,4</sup>, Kyle Wedgwood<sup>1,2,3</sup>, Krasimira Tsaneva-Atanasova<sup>1,2,3,4</sup>, Jon Brown<sup>5</sup>, and Marc Goodfellow<sup>1,2,3,4</sup>

<sup>1</sup>Living Systems Institute, University of Exeter <sup>2</sup>College of Engineering, Maths, and Physical Sciences, University of Exeter <sup>3</sup>Centre for Biomedical Modelling and Analysis, University of Exeter  
<sup>4</sup>EPSRC Centre for Predictive Modelling in Healthcare, University of Exeter <sup>5</sup>University of Exeter Medical School, University of Exeter

## Introduction

- The entorhinal cortex (EC) is a crucial component in spatial navigation systems and is one of the first areas to be affected in dementias featuring a tau pathology such as Alzheimer’s Disease.
- Electrophysiological recordings from principal cells of the EC (layer II stellate cells, SCs) demonstrate subthreshold oscillations in the theta (4-12 Hz) range and clustered action potential firing, in which two or more action potentials are fired in quick succession followed by a quiescent period.
- Experimental models of tau-mediated dementias have revealed changes in clustered action potential firing in the dorsal EC (1).
- Here, we present a model of EC SCs. A numerical bifurcation analysis is performed on the model to understand the dynamic mechanisms underlying clustering in the model and explore causes of changes in dynamics in dementia.

## Methods

We present a conductance based model with additive white noise on membrane potential, based on model of (2), given by  $C\dot{V} = I_{app} - \Sigma g_X \psi_X(V - E_X) + \sigma \eta(t)$ . Quantification of clustering is shown in Fig 1.

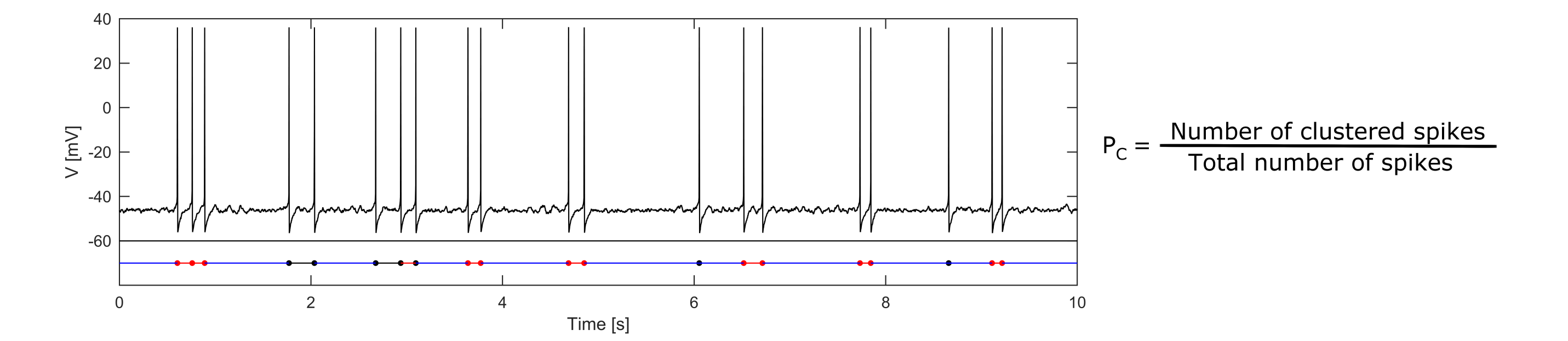


Fig. 1: Calculation of  $P_C$ . A cluster of spikes is defined as 2 or more spikes separated by an interspike interval (ISI) < 250 ms and preceded and followed by an ISI > 300ms. Red dots are clustered, black dots are not.  $P_C$  is the fraction of clustered spikes. Here,  $P_C = 13/20 = 0.65$ .

## Regimes of Clustering

The AHP and  $h$  currents are believed to be important in clustering, so  $P_C$  was calculated over a range of  $g_{AHP}$  and  $g_h$ . Regimes of realistic SC like clustering exist in the model (e.g. diamond in Fig 2).

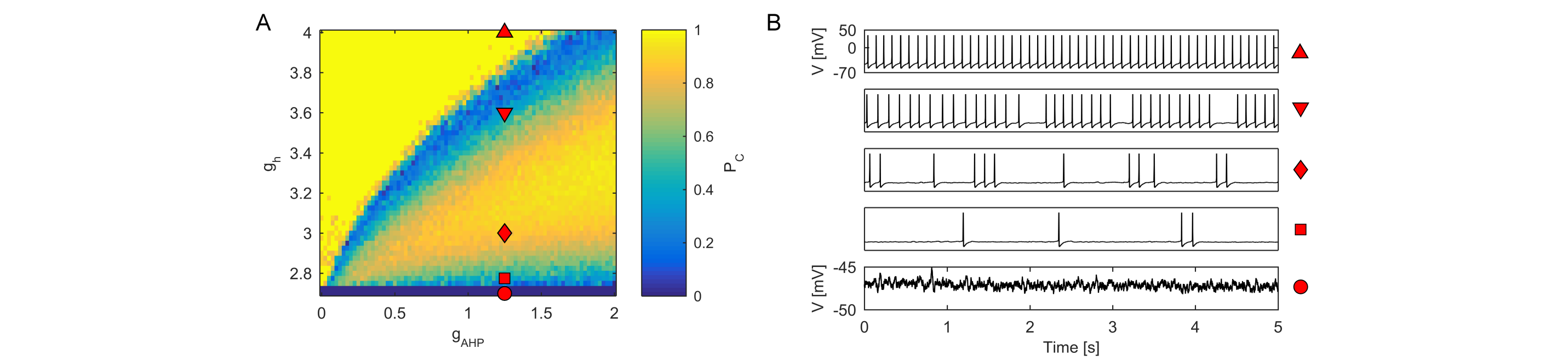


Fig. 2: (A) The value of  $P_C$  for different  $(g_{AHP}, g_h)$  regimes. (B) Example membrane potential traces at the parameter values indicated by the markers.

## Potential Mechanisms in Dementia

Fig 3 demonstrates example paths through parameter space from  $P_C$  of the wild type (WT) animals to  $P_C$  of the transgenic (TG) animals (1). Experimental data suggests there is no change in  $g_h$  and an increase in  $g_{AHP}$  in the TG animals (1). Therefore paths  $e$  and  $f$  are most likely. However, path  $e$  exhibits unrealistic SC dynamics. Path  $f$  is therefore a potential mechanism by which the changes in clustering seen in dementia may arise.

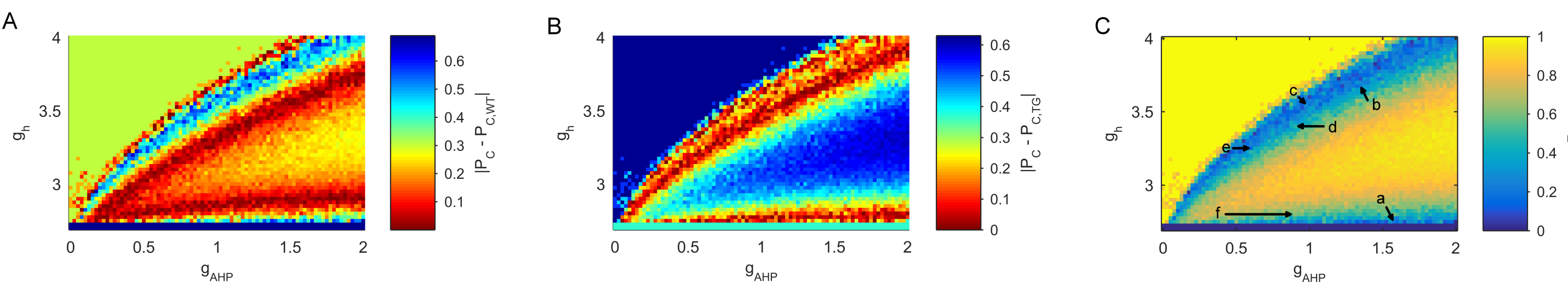


Fig. 3: (A) Magnitude of difference between  $P_C$  in model and  $P_C$  of WT data. Red means parameter regime is similar to that of WT data. (B) Similar to A, but for TG data. (C) Example paths from WT-like clustering to TG-like clustering.

## Clustering arises due to flip bifurcations

Removing the noise term ( $\sigma = 0$ ) from the model results in a system of ODEs on which a bifurcation analysis was performed. Deterministic clustering (periodic bursting) arises from tonic firing via a flip cascade through chaos. Flip bifurcations also take the system between regimes with different numbers of spikes per cluster.

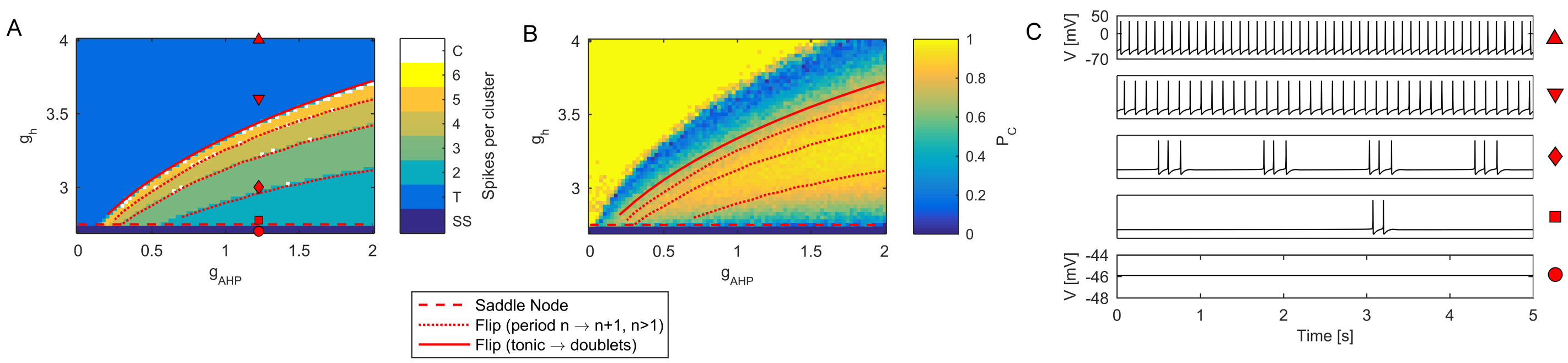


Fig. 4: (A) Heatmap showing different dynamic regimes in the deterministic system. Red lines show bifurcations. (B) Bifurcations in the deterministic system overlaid on the  $P_C$  heatmap for the stochastic system. (C) Example deterministic membrane potential traces at the parameter values indicated by the markers.

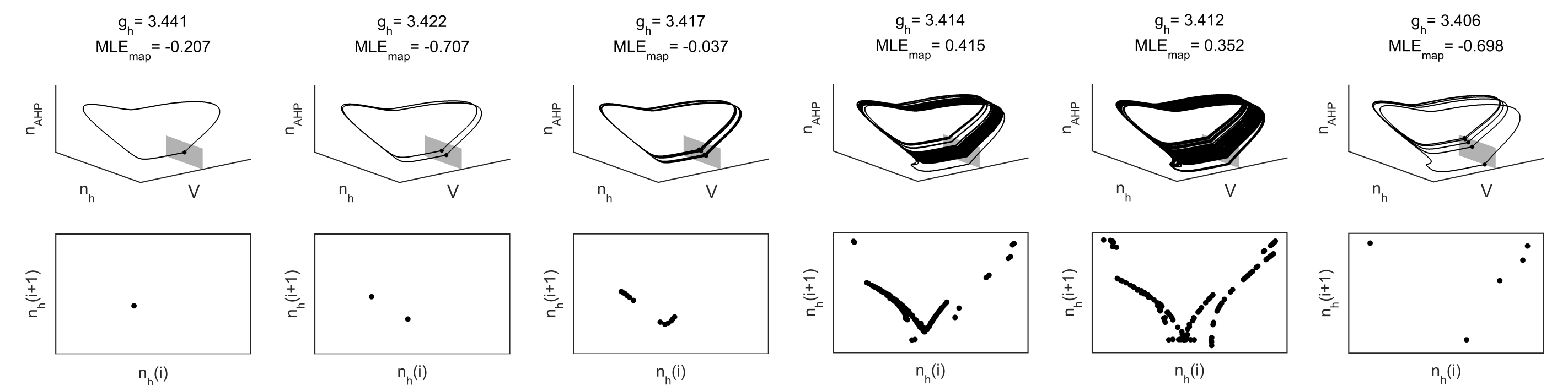


Fig. 5: Transition from tonic firing through chaos into period 5 clustered firing as  $g_h$  is decreased. Top row shows flows in the  $(V, n_h, n_{AHP})$  subspace about the Poincaré section  $V = 0$ . Bottom row shows the Poincaré return map for  $n_h$ . Values at the top show  $g_h$  and the maximum Lyapunov exponent on the map,  $MLE_{map}$ . If  $MLE_{map} > 0$ , the system is chaotic.

## Fast-slow analysis of clustering

Two slow variables drive bursting - activation of persistent sodium ( $m_{NaP}$ ) and inactivation of the slow A-type potassium current ( $h_{KAs}$ ). A two parameter bifurcation analysis of the fast sub-system demonstrated a region of bistability between steady state and tonic firing. In the full system, the evolution of the slow variables moves through this parameter space, driving the fast subsystem through a hysteresis loop and periodically switching between firing and steady state, resulting in bursting.

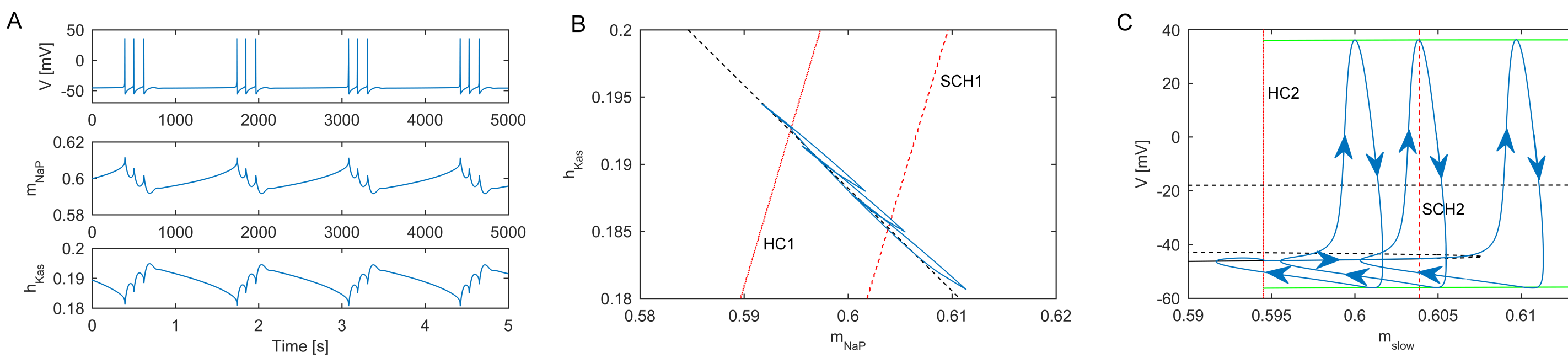


Fig. 6: (A) Deterministic dynamics of membrane potential and slow variables in a bursting regime. (B) Bifurcation analysis of the fast sub-system shows a homoclinic bifurcation (HC1) and a subcritical Hopf bifurcation (SCH1). The flow of the full system (blue) periodically moves across these bifurcations, resulting in periodic bursting. (C) Bifurcation analysis in which the slow subsystem is reduced to a single slow variable via a linear transformation.

## Subthreshold Resonance

In a subthreshold regime, the deterministic system is in a focus steady state with theta band resonant frequency. Noisy perturbations to this steady state give rise to a power spectral peak in the theta band consistent with data.

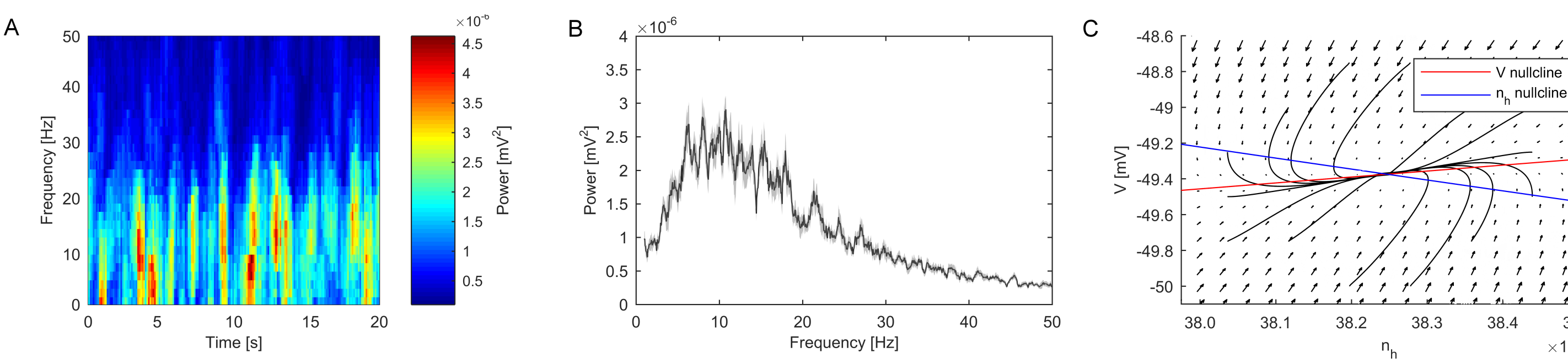


Fig. 7: (A) Spectrogram of example 20 second simulation in a subthreshold regime. (B) Average power spectrum of an ensemble of simulations. (C) The deterministic system is at a focus, meaning flows tend to 'spiral' into the steady state with resonant frequency in the theta band.

## References & Acknowledgements

- C.A. Booth, T. Ridler, et al. *J. Neurosci.*, 36(2):312-324, 2016.
- J.T. Dudman and M.F. Nolan. *PLoS Comput Biol* 5(2):e1000290, 2009.

The authors gratefully acknowledge the support of the Wellcome Trust (WT105618MA), EPSRC (EP/N014391/1), the Alzheimer’s Society DTC and the Garfield Weston Foundation.